ELSEVIER

Earth and Planetary Science Letters 202 (2002) 133–145

EPSL

www.elsevier.com/locate/epsl

Wavelet-based correlation (WBC) of zoned crystal populations and magma mixing

Glen S. Wallace *, George W. Bergantz

Department of Earth and Space Sciences, P.O. Box 351310, University of Washington, Seattle, WA 98195, USA

Received 22 January 2002; received in revised form 24 May 2002; accepted 28 May 2002

Abstract

Magma mixing is a common process and yet the rates, kinematics and numbers of events are difficult to establish. One expression of mixing is the major, trace element, and isotopic zoning in crystals, which provides a sequential but non-monotonic record of the creation and dissipation of volumes of distinct chemical potential. We demonstrate a wavelet-based correlation (WBC) technique that uses this zoning for the recognition of the minimum number of mixing, or open-system events, and the criteria for identifying populations of crystals that have previously shared a mixing event. When combined with field observations of the spatial distribution of crystal populations, WBC provides a statistical link between the time-varying thermodynamic and fluid dynamic history of the magmatic system. WBC can also be used as a data mining utility to reveal open-system events where outcrop is sparse. An analysis of zoned plagioclase from the Tuolumne Intrusive Suite provides a proof of principle for WBC.

Keywords: magma chambers; magma transport; crystal zoning; mixing; wavelets

1. Introduction

Igneous rocks often show evidence for repeated mixing of distinctive magmas and/or remobilization of within-chamber material [1,2]. In addition, the mixing processes can have a characteristic rise time as short as days to weeks [3,4], can occur intermittently throughout the history of a magma body (system) and may act as triggers to eruption [5]. But how are the scales of progressive mixing events preserved in the rock record, and how are they related to the transient response of a magma body to the repeated input of heat and mass? Given that the conditions represented in some mixed magmas and plutons often preserve an arrested or late, low-energy state, how can one look through this to understand the dynamic, earlier states? This issue is especially challenging in the case of composite-intermediate plutons, which provide much of the geological record of magmatic activity [6].

Mixing is fundamentally a process of particle (crystal) and melt gathering and dispersal followed by equilibration by diffusion (Fig. 1) [7,8]. Repeated mixing can also be conceptualized as the creation and dissipation of volumes of distinct chemical potential. In the mechanical sense, mix-

* Corresponding author.
E-mail address: gsw@u.washington.edu (G.S. Wallace).

0012-821X/02/$ – see front matter
PII: S0012-821X(02)00762-8

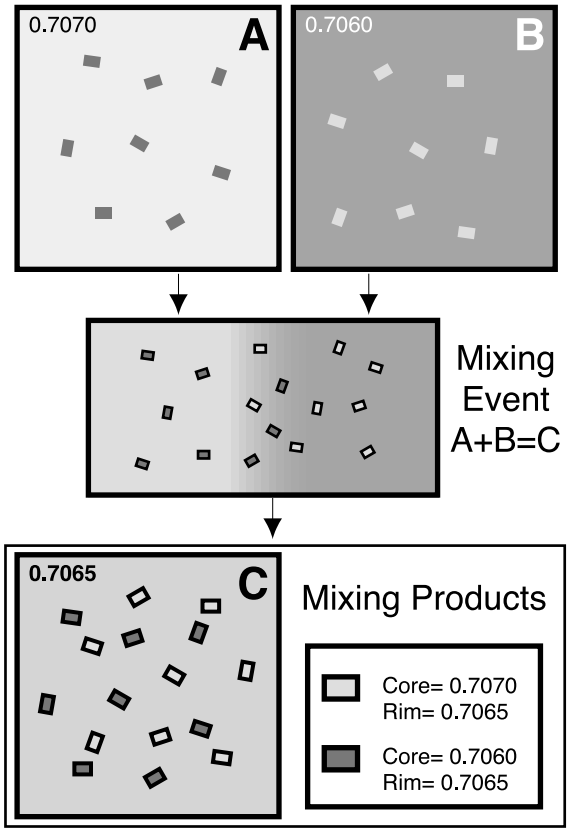

Fig. 1. Schematic diagram of the mixing of two distinctive magmas with arbitrarily assigned $^{87}Sr/^{86}Sr$ ratios. Black rims on crystals represent crystal growth during and after the mixing event. The output of the mixing event (A+B) is a mixed population (C) growing in a new hybrid melt.

ing can be defined in terms of the time-varying statistics of the dispersal of melt compositions and related to the buoyancy flux [9,10]. Regardless of how mixing is described, progressive mixing usually degrades the record of previous conditions in the melt phase and so the instantaneous melt composition may not reveal the temporal record of mixing.

However, in the crystalline record, mixing is sometimes preserved as complex resorption and zoning surfaces, melt inclusions and changes in the stable assemblage [11–17]. It has been proposed that crystals might provide an imperfect time-series and perhaps a 'stratigraphy' that might reveal progressive events in a magma chamber [18–24]. In this regard, one of the key obstacles to further progress is the absence of sufficient data density and a comprehensive set of analysis tools capable of quantitatively identifying the schedule of magma mixing, growth, fractionation and eruption in a time-stratigraphic framework. Notable conceptual progress has been made [6,25], but a quantitative framework for testable hypotheses of processes is still elusive.

In this paper, we demonstrate an objective data analysis approach to the study of crystal zoning that allows us to identify populations of crystals that have shared common thermodynamic environments. The central concept is that crystal zoning provides for a non-monotonic, but progressive time-series, and that magmatic events can be identified and correlated among crystals. We introduce the concept of wavelet-based correlation (WBC) which allows for simultaneous spatial–statistical inversion of all crystal zoning patterns for all crystals. This provides: (1) the minimum number of thermodynamic volumes involved in mixing and the populations of crystals that participated in a mixing event and, (2) when coupled with fluid dynamic models and geologic map data, estimates of relative motion between crystals and minimum residence times in portions of the system.

2. Crystal zoning

Crystals often display a compositional zoning that is a type of 'spatiotemporal' pattern, typical of many natural systems [26]. For example, the zoning of plagioclase, olivine, apatite and pyroxene crystals has been interpreted as progressively recording changes in magmatic environments [23,27–29].

Of special interest in magmatic systems is compositional zoning in plagioclase which has two characteristic scales [28]. Type I zoning is small-scale, generally in the range 1–10 μm, and has been shown to be the result of a deterministic process [26]. Type I zoning is interpreted to be controlled by a mismatch in the rates of crystal growth and diffusion of elements through the boundary diffusion layer, which causes an oscillatory depletion in major elements that is preserved as fine-scale zoning.

Type II zoning is wider, at scales in the range 3–100 μm and of greater amplitude, up to tens of mole percent anorthite. It likely reflects fluctuations in the local bulk-liquid composition, temperature, pressure and/or volatile content. In situ isotopic analyses within plagioclase grains show that type II zoning can be correlative with changes in isotopic ratios [30,31] and so, in these cases, cannot be the result of crystal boundary layer or complex growth effects. This provides support for the suggestion that type II zoning records progressive, but non-monotonic, changes in the magmatic environment which can be related to magma mixing processes.

In general, type I zoning in plagioclase does not correlate among grains, while type II zoning can be correlative between neighboring grains [32]. However, the superposition of types I and II zoning produces complex zoning patterns [33–35] that make it difficult to use zoning to interpret events recorded by suites of crystals. It has not generally been possible to uniquely interpret the combined effects of changes in temperature, pressure and composition within a magma chamber from the zoning of crystals. This is due to the fact that coupled component diffusivities and kinetics are not well known [17,26,36] and that crystals of differing ages will be gathered and dispersed during mixing. While it may be obvious from the final crystalline assemblage that mixing has occurred, understanding the mechanisms, extent and duration of mixing is not straightforward from complex zoning patterns.

An approach that may prove useful in extracting quantitative information is to examine crystal zoning in a signal processing framework. The signal processing framework is useful because it decomposes the complex expression of crystal zoning into component signals of distinct scales simultaneously for a very large number of crystals and in a way that is not possible in a rigorous sense with standard petrographic methods. One example of this approach is that chamber-wide melt evolution trends are generally preserved at a length scale approaching the entire core-to-rim length of the zoning profile, while processes operating at crystal melt interfaces are preserved at a length scale of a few micrometers. A signal processing approach explicitly allows for the separation and identification of these parts of the raw zoning data and thus provides the basis for correlation of distinct magmatic events between crystals.

If crystal zoning records progressive changes in the local thermodynamic environment, then crystals growing in the same thermodynamic environment should record the same progression of zoning features. Thus, identification of multiple zoning populations in a single sample can be geologically interpreted as a convergence of crystals from distinctive thermodynamic environments [37]. Once the full range of scales of zoning is characterized for a mineral system, it should be possible to compare the transport history of crystals in the context of integrated changes in the thermodynamic environment. However, in order to compare zoning profiles in a signal processing framework, a quantitative technique that can resolve the locations of features in zoning profiles is needed.

3. The continuous wavelet transform (CWT)

An objective data analysis technique that is well suited for structured data such as crystal zoning is the CWT [38,39]. The wavelet transform separates the components of the zoning without losing information as to their location within the crystal. One can then look at the components without the complications of their inherent superposition. Previously, Fourier-based methods have been used to identify the dominant amplitudes of crystal zoning [17]. The Fourier-based methods make the implicit assumption that the zoning is periodic, or stationary, and so represents the zoning in terms of a repeating, orthogonal set of basis functions such as sines and cosines. However, these assumptions preclude the resolution of the distribution of frequency components in the spatial domain, such as the particular location in the crystal where dominant frequencies occur. Hence, Fourier-based methods cannot serve as a technique for time-correlative analysis among crystals. The CWT is a departure from Fourier-based techniques, in that it can resolve time–frequency

relationships in non-periodic, or non-stationary, structured data. Reviews of the wavelet technique with geophysical applications can be found in [39–42]; there are also tutorials available on the World Wide Web.

The CWT represents a signal, such as a profile of crystal zoning, by comparing the zoning signal to a reference function called the mother wavelet function (referred to hereafter as the wavelet) over a range of translations and scales, thereby allowing localized, multi-scale resolution (Fig. 2). For one-dimensional data analysis, the CWT has the form:

$$\mathrm{CWT}(s,\tau) = \frac{1}{s}\int f(x)\,\phi\left(\frac{x-\tau}{s}\right)\mathrm{d}x \qquad (1)$$

where $f(x)$ is the zoning profile (it is implied that x is the coordinate from core to rim), ϕ is the wavelet, τ is a translation term and s is the scale. For discrete data, iteration over a range of translations and scales appropriate to $f(x)$ results in a matrix of wavelet coefficients ($\mathrm{CWT}_{s,\tau}$). Each wavelet coefficient is a calculation of the CWT at the specified scale and translation. The scale, or dilation, of the wavelet determines the width and frequency response of the wavelet. Translation determines where the wavelet is aligned relative to the zoning profile. An intuitive way to view wavelet coefficient values is as a measure of the similarity between $f(x)$ and ϕ at a particular dilation and location in $f(x)$. Positive wavelet coefficients result from peaks in the zoning profile and negative coefficients result from valleys, or minima in $f(x)$. Thus the wavelet can have a dual role; it re-represents the signal as a collection of component signals at a certain scale and also acts as a probe for features in the data with morphologies similar to the mother wavelet.

In summary, the advantage of the wavelet transform is that it decomposes the zoning profile into a set of component profiles that can better reveal the underlying structure in the zoning, while not losing the information of the location of the components in the original zoning pattern. This allows for the selective recognition and comparison of spatiotemporal features among crystals.

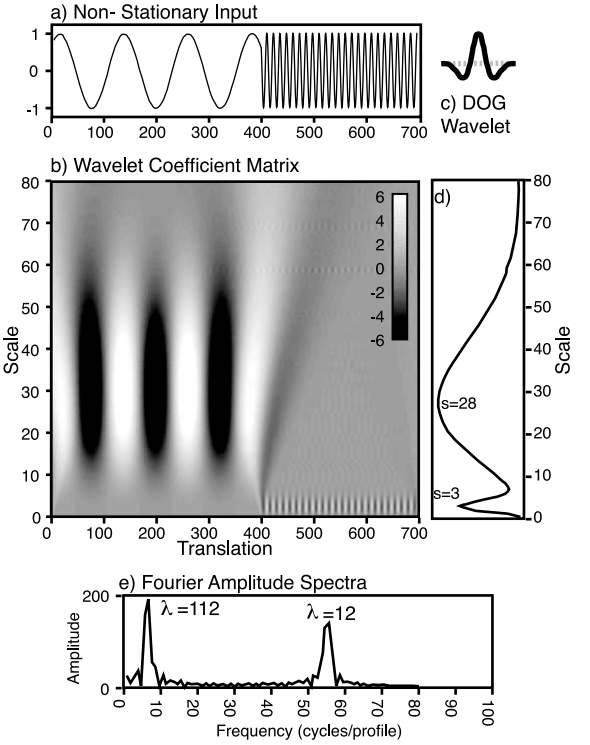

Fig. 2. Example wavelet analysis of a non-stationary signal. (a) The input has two sections with periods of 112 and 12 points. The signal is not strictly periodic because the frequency content of the signal changes across the signal. (b) Wavelet coefficient matrix. Coefficients are calculated with the DOG wavelet as the mother wavelet function. (c) Positive and negative wavelet coefficients correspond to peaks and valleys in the input data. The shift in scale corresponds to a change in frequency in the input data at 400. (d) For comparison purposes, the dominant scales in the signal determined by wavelet analysis are shown in a plot of scale vs. average coefficient values, with maxima at scales $s=3$ and $s=28$. An empirically determined 4:1 scaling relationship for the DOG wavelet ties to Fourier analysis with the Fourier amplitude spectra of the sample input showing dominant periods of $\lambda=12$ and $\lambda=112$ points. (e) Peaks are sharper in (e) because the basis function in Fourier analysis matches the sample signal. The key point of this figure is comparison between (b) and (e). Fourier analysis gives excellent frequency resolution, but offers no information on where in a signal specific frequencies are located. Wavelet analysis provides information on the dominant frequencies and their location in a signal. For the purposes of WBC, only the information in (b) is used.

4. WBC

One objective of the wavelet analysis is to identify populations of crystals that have some shared history both within a sample and/or between samples which can be from the same outcrop or separate outcrops. To determine the populations of zoned crystals, WBC addresses the questions: what crystals have similar zoning patterns and where are those patterns the same between profiles and samples? This provides the basic criteria for the definition of crystal populations and also where in their zoning profile crystals began growing in a common environment. WBC is implemented in four steps.

4.1. Step one: data acquisition

The uncertainties in the WBC analysis will depend on the data quality, which has two aspects: the inherent uncertainties in the data gathering technique, and the respective orientation, geometry and nucleation time of the individual crystals. Ginibre et al. [17] review the techniques for the characterization of compositional zoning and their associated uncertainties. Pearce and Kolisnik [43] review the criteria for crystals that will be optimal for zoning study. They should be euhedral, nearly center-cut, and with zoning nearly perpendicular to the plane of the thin section. In practice, it is difficult to obtain optimal grain orientations without resorting to prohibitively laborious methods and strict criteria that bias selection towards a restricted size range and crystal shape.

This selective bias can result in incomplete sampling of a crystal population with a diverse crystal size distribution. Off-center profiles are readily measured and are more likely to provide a characteristic sampling of a population, but are difficult to compare due to geometric effects. The range of geometric effects generally reduces to profile stretching and/or removal of information from the crystal core. If the actual orientation and position of a random profile are known relative to the optimal section, it is trivial to stretch and translate a profile for comparison. However, this information is rarely, if ever, available. We have developed an adaptive profile normalization technique that objectively translates and stretches profiles in preparation for wavelet analysis. In short, the technique generates an array of possible stretching and translations for each pair of profiles. Then, the best fit for that pair of crystals is determined by standard correlation and used in WBC. Preliminary Monte Carlo experiments indicate that this approach improves the accuracy of WBC by about 30%, as compared to WBC of profiles with no normalization.

4.2. Step two: wavelet transformation

The target output of the wavelet transformation step is a matrix of wavelet coefficients, which represent only the zoning widths of interest for the geologic analysis. As discussed above, these are calculated with the wavelet transform. Each mother wavelet function has a scaling function that can be used to relate scale to a wavelength. This relationship, in conjunction with observational, theoretical or empirical knowledge of zoning types, is used to determine what range of scales should be used in the wavelet analysis of zoning profiles, such that only the zoning type of interest is represented in the final wavelet coefficient matrix (Fig. 4). Alternatively, the scale range of interest can be extracted from a wavelet coefficient matrix after wavelet analysis over a broader range of scales, but this results in unnecessary calculations.

The choice of the appropriate wavelet function for a given application is not obvious as many wavelets may give qualitatively similar results. Because wavelet coefficients are dependent on the similarity between ϕ and $f(x)$, the wavelet should be matched to the spectral properties of the signal. However, there has been little analysis of how best to match a particular wavelet for a particular spatiotemporal signal. Leblanc [44] proposes a combination of power spectrum analysis and other statistical tools in evaluating the selection of a wavelet for analysis when data recovery from wavelet coefficients is required, but no widely applicable guidelines have been identified. For the analysis of plagioclase zoning profiles, we employ the Mexican Hat, or Derivative of Gaussian

(DOG) wavelet (Fig. 2), defined as:

$$\phi(x) = \left(\frac{2}{\sqrt{3}}\pi^{-1/4}\right)(1-x^2)e^{-x^2/2} \quad (2)$$

Our wavelet selection is based on two criteria: (1) the DOG wavelet has the best resolution in WBC correlation coefficients in duplicate WBC analyses with Haar, Morlet, DOG and Daubechies wavelets; (2) the DOG has a narrow spectral range and a single well-defined peak in the spatial domain, providing better sensitivity to abrupt features in zoning profiles.

The ends of profiles produce edge effects that reduce resolution and produce spurious results when used in data correlation analysis. Edge effects can be mitigated in a number of ways. In traditional Fourier analysis, data are padded with either a periodic, symmetric or zero extension of the signal. In addition to generating distortion at the edges of padding segments in wavelet analysis, these padding routines implicitly assume periodicity and are not well suited for wavelet analysis of non-stationary zoning profiles. Padding zoning profiles with the first and last measured values generates the smallest edge effects and is chosen for the analyses presented in this paper.

4.3. Step three: correlation and cluster analysis

Two criteria for quantitative data comparison are correlation and covariance. Both compare how pairs of points from profiles behave relative to the profile means and provide a measure of the similarity of pairs of profiles. The correlation coefficient for two data sets x and y is defined as:

$$r = \frac{\mathrm{cov}(x,y)}{\sqrt{\mathrm{var}(x)}\sqrt{\mathrm{var}(y)}} \quad (3)$$

Where variance and covariance are defined as:

$$\mathrm{var}(x) = \frac{1}{N-1}\sum_{i=1}^{N}[x_i-\overline{x}]^2 \quad (4)$$

and:

$$\mathrm{cov}(x,y) = \frac{N\sum_{i=1}^{N}x_iy_i - \sum_{i=1}^{N}x_i\sum_{i=1}^{N}y_i}{N(N-1)} \quad (5)$$

Where $\overline{x}$ is the arithmetic mean of the data set and N is the number of data points. In situations where the variance of profiles is likely to be different the use of correlation is preferable. However, when the magnitude of similarity is important, covariance is a useful tool, but perhaps less intuitive to interpret. Where profiles have similar var-

Table 1
Correlation coefficients

	Kcp1	Kcp2	Kcp3	Kcp5	Kcp6	Kcp7	Kcp8	Kcp9	Kcp11	Khdp14	Khdp15	Khdp16	Khd17	Khdp18	Khdp19	Khdp20
Kcp1	**1.00**	0.93	0.85	0.44	0.81	0.30	0.87	0.63	0.64	0.46	0.68	0.52	0.61	0.21	0.85	0.40
Kcp2	*0.54*	**1.00**	0.68	0.32	0.11	0.33	0.86	0.36	0.82	0.64	0.71	0.14	0.86	0.84	0.69	0.61
Kcp3	*0.12*	*0.20*	**1.00**	0.75	0.67	0.42	0.81	0.50	0.93	0.94	0.79	0.09	0.76	0.78	0.80	0.78
Kcp5	*0.75*	*0.51*	*0.36*	**1.00**	0.76	0.65	0.60	0.81	0.90	0.36	0.52	0.79	0.66	0.45	0.91	0.46
Kcp6	*0.60*	*0.46*	*-0.02*	*0.35*	**1.00**	0.45	0.57	0.88	0.70	0.46	0.48	0.64	0.88	0.77	0.31	-0.42
Kcp7	*0.71*	*0.52*	*0.26*	*0.75*	*0.47*	**1.00**	0.68	0.37	0.90	0.54	0.42	0.79	0.48	0.61	0.86	0.44
Kcp8	*0.64*	*0.58*	*-0.02*	*0.61*	*0.71*	*0.66*	**1.00**	0.68	0.87	0.76	0.67	0.62	0.84	0.51	0.69	0.85
Kcp9	*0.64*	*0.58*	*0.17*	*0.76*	*0.67*	*0.63*	*0.71*	**1.00**	0.80	0.13	0.40	0.56	0.76	0.25	0.83	0.82
Kcp11	*0.57*	*0.54*	*-0.21*	*0.36*	*0.62*	*0.52*	*0.84*	*0.67*	**1.00**	0.61	0.59	0.88	0.86	0.75	0.81	0.74
Khdp14	*0.76*	*0.60*	*0.17*	*0.81*	*0.50*	*0.82*	*0.75*	*0.73*	*0.61*	**1.00**	0.55	0.89	0.62	0.35	0.49	0.69
Khdp15	*0.75*	*0.64*	*0.03*	*0.72*	*0.68*	*0.75*	*0.86*	*0.76*	*0.77*	*0.84*	**1.00**	0.47	0.43	0.66	0.63	0.20
Khdp16	*0.16*	*0.49*	*-0.24*	*0.30*	*0.62*	*0.54*	*0.69*	*0.62*	*0.78*	*0.58*	*0.71*	**1.00**	0.71	0.79	0.39	0.71
Khdp17	*0.79*	*0.64*	*0.05*	*0.74*	*0.63*	*0.78*	*0.80*	*0.73*	*0.75*	*0.85*	*0.87*	*0.66*	**1.00**	0.59	0.72	0.51
Khdp18	*0.72*	*0.52*	*0.21*	*0.68*	*0.38*	*0.61*	*0.55*	*0.62*	*0.28*	*0.68*	*0.66*	*0.47*	*0.66*	**1.00**	0.38	0.26
Khdp19	*0.48*	*0.56*	*0.03*	*0.28*	*0.52*	*0.41*	*0.59*	*0.42*	*0.58*	*0.55*	*0.67*	*0.24*	*0.69*	*0.77*	**1.00**	0.38
Khdp20	*0.74*	*0.70*	*0.16*	*0.69*	*0.67*	*0.74*	*0.81*	*0.71*	*0.73*	*0.85*	*0.88*	*0.40*	*0.88*	*0.70*	*0.74*	**1.00**

Correlation coefficients of zoning profiles from Kcp and Khdp, see text. Values above the diagonal are calculated using the WBC technique while those in italic below the diagonal are standard correlations from the raw zoning profiles. Shaded region indicates correlation of grains between samples. WBC was implemented in the scale range 5:20 using the DOG wavelet, as shown in Fig. 2.

iances, covariance and correlation will produce similar results.

Standard correlation and WBC are sensitive to different components of the signal and therefore generate different correlation coefficients for the same set of profiles (Table 1). Normal zoning trends dominate standard correlation because the deviation from the mean and variance associated with normal zoning is larger than any other component of the signal. Because WBC selects only the type II component of the zoning signal, WBC correlation coefficients are not affected by longer wavelength zoning trends.

Because population determination is based on correlation, significance levels for correlation values are needed for reference. Independently measured profiles from the same grain generally correlate around the 0.95 level using WBC, defining the upper end of reasonably expected correlations. We determined the minimum significant correlation by Monte Carlo WBC of 200 synthetic zoning profiles. Correlations above 0.80 are significant at the 95th percentile. Correlation values that fall below the significance level cannot be distinguished from a random population and are grouped as non-correlative.

Cluster analysis provides a framework for the determination of crystal zoning populations on the basis of their correlation coefficients from WBC. The number of populations determined by cluster analysis for a single sample is a measure of heterogeneity of the profiles. Because heterogeneity is a result of mixing of crystal populations, cluster analysis provides a measure of the complexity of the mixing history. Cluster analysis collects correlation coefficients into groups that are similar at or above a correlation threshold that is set between one and the minimum significant correlation. A minimum of two crystals are required to define a population at the given level of correlation, which implies that the maximum number of populations that can be resolved is limited to half the number of analyzed profiles.

Neither correlation nor covariance yields information on what segments of the zoning profiles are similar or what type of feature is controlling correlation. Both aligned peaks and aligned flat portions of zoning profiles will increase correlation. In order to resolve the detailed progression of mixing, a framework for the identification of where, within pairs of zoning profiles, grains correlate is required.

4.4. Step four: mixing phylogeny

One of the assumptions of WBC is that crystals growing in different environments are unlikely to develop (nearly) identical zoning profiles and those that are growing in the same environment will. Implicit in this assumption is that if two grains are brought together, they will have identical rims and different cores, and the transition between these two zoning segments marks the convergence of the crystals to a common growth history. This convergence point in zoning profiles is identified on a pair-by-pair basis by a decrease in cross-correlation on a rim-to-core traverse (Fig. 3a). Cross-correlation is determined by calculating the correlation between windowed segments of the wavelet coefficient matrices along the rim-to-core traverse. When this process is repeated for many pairs of crystals, it may be seen that individual crystals have multiple convergence points, corresponding to multiple gathering events with other individual or sets of crystals.

The synthesis of convergence points for all crystal pairs is a phylogeny diagram showing the growth-normalized history of gathering events for the population (Fig. 3b). Each convergence point in a cross-correlation diagram is a branching point in the phylogeny diagram. Therefore, the number of branching points in a phylogeny diagram is the minimum number of gathering events for that set of crystals. Because the phylogeny diagram is based on cross-correlation and convergence, it offers a different measure of the mixing history than cluster analyses in that it incorporates a specific time-stratigraphic history instead of a generalized heterogeneity (Fig. 3c). The number of populations in cluster analysis is qualitatively related to the number and distribution of branching points in the mixing phylogeny (Fig. 3c). Cross-correlation diagrams yield similar information to cross-wavelet spectra, a similar wavelet-based analytical tool used in seismic tomography [41,42].

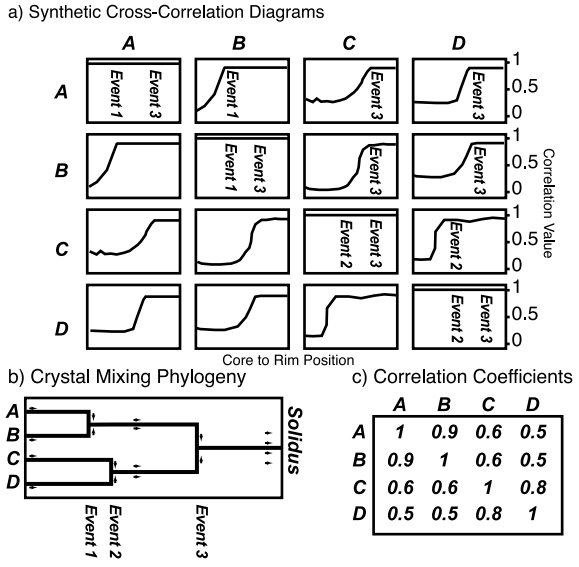

Fig. 3. Mixing phylogeny based on WBC analysis of a hypothetical set of crystals A, B, C and D that converge through mixing events 1, 2 and 3. (a) Events are identified in each crystal by a decrease in cross-correlation on rim-to-core traverses and synthesized into a phylogeny diagram (b). (c) Hypothetical correlation coefficients are simply scaled by the amount of shared history between grains. Correlation coefficients define two populations, which only require a minimum of one mixing event, but do not offer information on the possibility of a larger number of mixing events. At the initial condition in the phylogeny, each of the crystals is in a different environment. At event 1, A and B are brought together, which is indicated in the cross-correlation diagrams by a transition to higher correlation, while C and D show no change because they are not brought together by the event either because they were not involved, or they did not record the event. At event 2 in the phylogeny, C and D are brought together and have a corresponding transition to higher correlation in the cross-correlation diagrams. A and B continue to grow together, but do not record event 2. At event 3, all crystals converge, as indicated by C and D transitioning to higher correlation with A and B in cross-correlation diagrams.

5. Integrating WBC with geology

WBC can identify populations of crystals that have shared some common thermodynamic history. Recall that a single crystal may have belonged to many populations during its growth, as a consequence of dispersal during magmatic processes. Considered as an end member, if magma is continuously well mixed and homogenized, all samples from that system should produce internally consistent WBC correlation and phylogeny results because all crystal populations will be evenly distributed throughout the magma volume. Conversely, heterogeneity in WBC populations and phylogeny between samples lead to an interpretation of a heterogeneous environment where independent magma volumes were combined. Thus the spatial distribution of populations, as expressed by the distribution of zoned crystals in outcrop, provides a measure of preserved length scale, geometry and effectiveness of mixing events [45]. By mapping the relative positions and styles of zoning of crystals that form the populations that are dispersed, one can estimate the amount of transport that has taken place. The recognition of particle paths by the identification of shared transport and subsequent dispersal by many particles is called 'Lagrangian trajectory analysis' [46].

This approach can only work in igneous rocks that have remained mechanically connected. By this we mean that they have not undergone complete fragmentation and dispersal by eruption. Eruption destroys information of the relative position of adjoining elements in the magma chamber and so proximity in deposits of fragmented rocks does not imply proximity within the magma chamber. For this reason plutonic rocks and effusively erupted volcanic rocks offer the best opportunities for the application of WBC.

One application of the 'data mining' utility of WBC is to the geological history of magmatic systems that are sparsely represented in the rock record. The premise is that the information content of an outcrop is not necessarily related to the size of that outcrop. A modestly sized outcrop may contain enough crystal populations that many open-system events can be recognized, events that may have influenced the entire magmatic system. The application of WBC, in conjunction with emerging microanalytical dating techniques [47], may aid the identification of the recurrence interval of eruptions and open-system events in volcanic systems, where much of the edifice has been removed by erosion or eruption, a common occurrence in volcanic arcs.

One expression of the processes of mixing is the amplitude of compositional zoning. A corollary of

WBC is that it can only identify distinct crystal gathering events whose duration is longer than the sampling time of the mineral. The duration of a mixing event is controlled by the initial volume of material and the buoyancy flux, which is a function of the kinematics of the flow field. The reaction or sampling rate is controlled by the kinetics of the resorption rate or the growth rate at the crystal–melt interface. The ratio of the characteristic time of the fluid dynamics to the reaction rate is known as the Damköhler number [8]. If the reaction rate goes to zero, the Damköhler number becomes infinite and composition can be considered to be a state variable, and the crystal will record all local chemical changes during mixing. Conversely, at very slow reaction rates, the Damköhler number is vanishing, and the crystals will not record the details of the mixing event, but only the average compositions that are present after complete homogenization. For a Damköhler number of about unity, both the finite-rate kinetics of the reaction and the details of the flow field must be considered explicitly as an evolving process. The uncertainties in the application of WBC increase as the Damköhler number drops below a value of order unity, indicative of a time-lag between a mixing event and its appearance in crystal zoning. In summary, the preservation of sharp, large-amplitude fluctuations, such as type II zoning in plagioclase, indicates a large Damköhler number and means either that the rate of mixing was slow and that compositional gradients persisted in the mixed system, or that the reaction rate of the plagioclase grain was rapid compared to the mixing time. If reaction rates can be independently assessed, minimum mixing times can be estimated.

We close this discussion with a number of caveats in the application of WBC to geological examples. Mixing events may not be distinctly recorded in zoning profiles if their chemical effect is close to the scale of type I zoning (or equivalent in minerals other than plagioclase), if multiple events occur close enough in time to be resolved as a single event, or if the zoning is simply removed by resorption. We have developed a Monte Carlo approach which we will use to determine the effects of variable crystal size, signal noise, off-center sections and progressive new-crystal nucleation on WBC correlation and phylogeny results. The objective of the Monte Carlo approach is to generate objective guiding criteria for the number and quality of grains that must be analyzed for reasonable confidence in geologic interpretations. Results of the Monte Carlo experiments will be presented elsewhere.

6. Application of WBC to an example of mixing in the Tuolumne Intrusive Suite (TIS)

Plutonic suites of intermediate composition offer the opportunity to demonstrate WBC. They often manifest mixing and mingling of distinct compositional domains with conspicuous crystal transfer [37]. A plutonic example is chosen because the spatial relationships between samples are preserved. We will demonstrate the use of WBC on a data set from the Cretaceous TIS in the Sierra Nevada of California. The TIS was selected because it has been well characterized and offers independent evidence of magma mixing and mingling [48–50].

The concentrically zoned TIS is composed of five plutonic units, from the inner, youngest unit: the Johnson Porphyry (Kjp), the Cathedral Peak Granodiorite (Kcp), the Half Dome Porphyritic Granodiorite (Khdp), the Half Dome Granodiorite (Khd) and the equivalent Glen Aulin and Kuna Crest Tonalites (Kga and Kkc, respectively). These units are divided on the basis of texture, major and accessory mineral assemblages and contact relationships [51].

The aim of our field study is to assess whether WBC can reveal mass transport, or mixing, between the Khd and Kcp to create, or at least contribute to, the intervening Khdp. Mechanical and chemical mixing between units of the TIS is interpreted from several lines of evidence, including: geochemical evidence: overlapping whole rock composition trends between units [48]; kinematic evidence: textural evidence in felsic enclaves for hypersolidus transfer, aplite dikes transporting pods of Kcp into Khdp, and gradational contacts; isotopic evidence: increasing $^{87}Sr/^{86}Sr$ across the Khd–Khdp–Kcp contact zone [52].

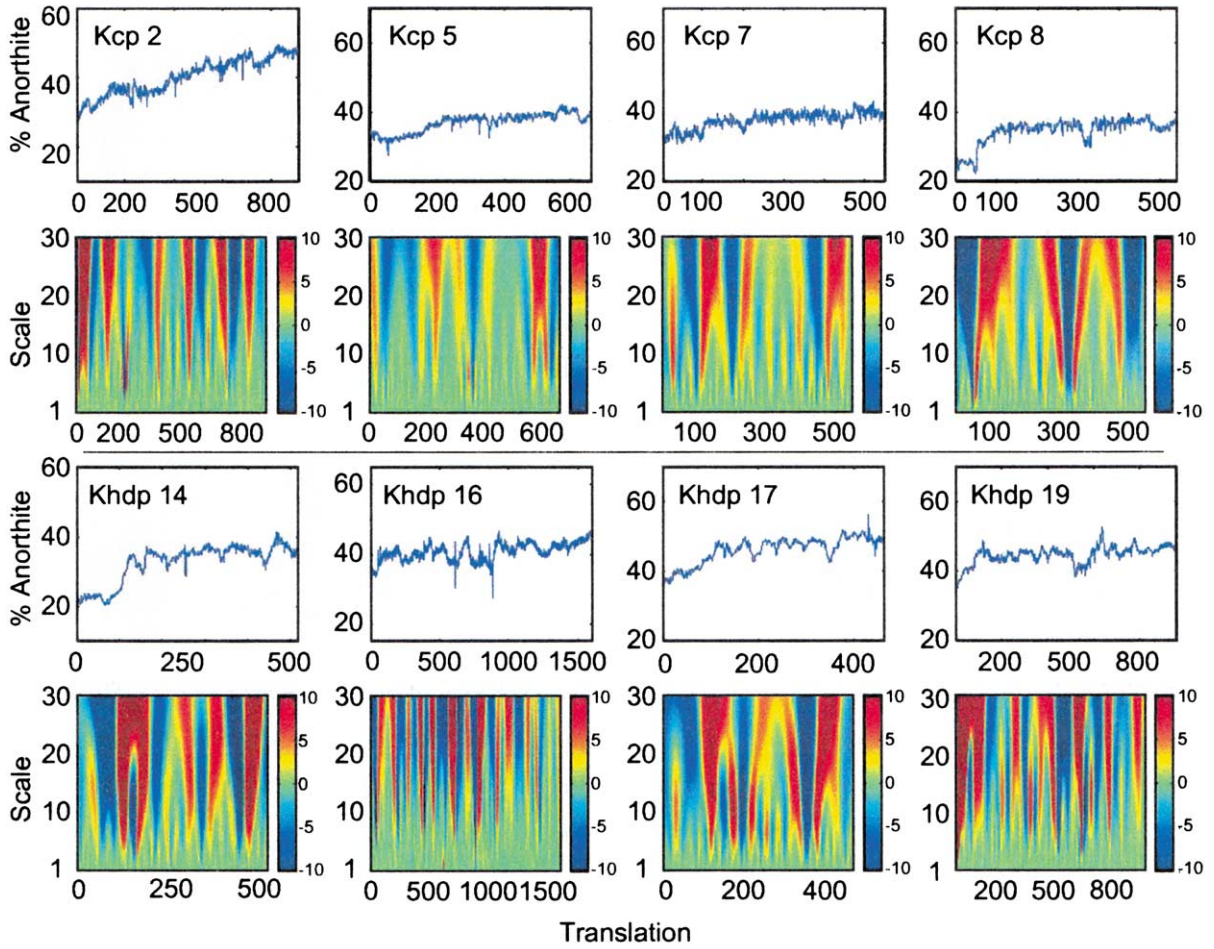

Fig. 4. Selected zoning profiles and wavelet coefficient matrices from the Kcp and Khdp, as discussed in text. Scale bars show the magnitude and sign of wavelet coefficient matrix values. Positive and negative values on wavelet coefficient matrices correspond to peaks and valleys in the data, respectively, as in Fig. 2. These profiles have not been adaptively normalized, so visual inspection of similarity between wavelet coefficient matrices may not be strictly meaningful for comparison against correlation coefficients presented in Table 1.

6.1. Analysis

Two samples were collected from the TIS for analysis: the first from a gradational portion of the Khd–Khdp contact (sample Khdp), and a second from the main phase Kcp, 2.7 km away (sample Kcp). Anorthite profiles were measured from plagioclase grains using a calibrated BSE imaging technique modified from Ginibre et al. [17] at an initial resolution of about 600 points per profile and subsequently adaptively normalized on a pair-by-pair basis, as discussed above. All grains show stepped, oscillatory zoning superposed on a normal zoning trend in the range An_{50}–An_{24} (Fig. 4). Wavelet coefficient matrices were calculated with the DOG wavelet over the scale range 5–25. This scale range corresponds to resolutions of 20–100 pixels, which is well above the minimum sampling requirement for wavelet analysis. Correlations of wavelet coefficient matrices are generally high between Kcp grains and patchy between Khdp grains (Table 1). A number of

grains have statistically significant correlations between Kcp and Khd. Correlation between samples occurs less often than correlation within Kcp, but more often than correlation within Khdp. Cross-correlation diagrams are not shown because the data set is too small to reliably construct a phylogeny diagram.

The WBC results show a slightly greater degree of heterogeneity at the Khd–Khdp contact than in the Kcp. The larger number of crystal populations is consistent with an interpretation that the intermediate unit, Khdp, is composed of some crystals that may have a complex transport history. The heterogeneity of the crystal population in Khdp is consistent with mingling of at least two crystal populations. This may be due to mixing within Khdp, introduction of plagioclase grains from a third reservoir such as mafic or felsic enclaves, or mass transfer between adjoining units. The observation of schlieren and the heterogeneous distribution of potassium feldspar megacrysts in the Khd–Khdp contact zone indicate mingling with length scales of at least tens of meters. This is also consistent with evidence for hypersolidus interaction between units and is consistent with the correlation of Khdp grains with grains from Kcp (Table 1).

7. Conclusions

WBC provides a new technique to investigate the record of mechanical mixing in magmatic systems by the identification of linked crystal populations. Integration of WBC and in situ microanalytical isotopic and geochemical measurements presents a framework for mutually testable physical and chemical models of magmatic systems. Preliminary results from the TIS indicate that WBC is capable of making crystal population determinations that are in agreement with other geological evidence. Populations defined by mean correlation values indicate that plagioclase crystals in the analyzed samples have complex transport histories and are consistent with independent interpretations of both mechanical and chemical mixing in the TIS.

Acknowledgements

This research has been supported by NSF Grants EAR-9805336 and EAR-0106441. Insightful reviews by J. Miller, J. Tepper and D. Yuen in addition to reviews on a previous version by J. Hammer, M. Coombs and L. Mastin were very helpful. Discussions with J. Davidson, K. Knesel, V. Kress and C. Ginibre and assistance in microprobe and BSE analyses by S. Kuehner are appreciated. *[SK]*

References

[1] J.P. Davidson, F.J. Tepley III, Recharge in volcanic systems: Evidence from isotope profiles of phenocrysts, Science 275 (1997) 826–829.
[2] D.M. Pyle, M. Ivanovich, R.S.J. Sparks, Magma-cumulate mixing identified by U–Th disequilibrium dating, Nature 331 (1988) 157–159.
[3] M.L. Coombs, J.C. Eichelberger, M.J. Rutherford, Magma storage and mixing conditions for the 1953-68 eruption of Southwest Trident volcano, Katmai National Park, Alaska, Contrib. Mineral. Petrol. 140 (2000) 99–118.
[4] M. Nakamura, Continous mixing of crystal mush and replenished magma in the ongoing Unzen eruption, Geology 23 (1995) 807–810.
[5] G.W. Bergantz, R.E. Breidenthal, Non-stationary entrainment and tunneling eruptions: A dynamic link between eruption processes and magma mixing, Geophys. Res. Lett. 28 (2001) 3075–3078.
[6] R. Bateman, The interplay between crystallization, replenishment, and hybridization in large felsic magma chambers, Earth Sci. Rev. 39 (1995) 91–106.
[7] J. Baldyga, J.R. Bourne, S.J. Hearn, Interaction between chemical reactions and mixing on various scales, Chem. Eng. Sci. 52 (1997) 457–466.
[8] J.M. Ottino, The Kinematics of Mixing: Stretching, Chaos, and Transport, Cambridge University Press, Cambridge, 1989, 354 pp.
[9] C.M. Oldenburg, F.J. Spera, D.A. Yuen, G. Sewell, Dynamic mixing in magma bodies: Theory, simulations and implications, J. Geophys. Res. 94 (1989) 9215–9236.
[10] A.M. Jellinek, R.C. Kerr, Mixing and compositional stratification produced by natural convection 2. Applications to the differentiation of basaltic and silicic magma chambers and komatiite lava flows, J. Geophys. Res. 104 (B4) (1999) 7203–7218.
[11] M.J. Hibbard, The magma mixing origin of mantled feldspars, Contrib. Mineral. Petrol. 76 (1981) 158–170.

[12] G.T. Nixon, T.H. Pearce, Laser-interferometry study of oscillatory zoning in plagioclase: The record of magma mixing and phenocryst recycling in calc-alkaline magma chambers, Iztaccihuatl volcano, Mexico, Am. Mineral. 72 (1987) 1144–1162.
[13] M.L. Stewart, A.D. Fowler, The nature and occurrence of discrete zoning in plagioclase from recently erupted andesitic volcanic rocks, Montserrat, J. Volcanol. Geotherm. Res. 106 (2001) 245–255.
[14] J.A. Stimac, T.H. Pearce, Textural evidence of mafic-felsic magma interaction in dacite lavas, Clear Lake, California, Am. Mineral. 77 (1992) 795–809.
[15] D.M. Robinson, C.F. Miller, Record of magma chamber processes preserved in accessory mineral assemblages, Aztec Wash pluton, Nevada, Am. Mineral. 84 (1999) 1346–1353.
[16] J. Tepper, S. Kuehner, Complex zoning in apatite from the Idaho batholith: A record of magma mixing and intracrystalline trace element diffusion, Am. Mineral. 84 (1999) 581–595.
[17] C. Ginibre, A. Kronz, G. Worner, High-resolution quantitative imaging of plagioclase composition using accumulated back-scattered electron images: New constraints on oscillatory zoning, Contrib. Mineral. Petrol. 142 (2002) 436–448.
[18] G.T. Nixon, Petrology of the younger andesites and dacites of Iztaccihuatl volcano, Mexico: I. Disequilibrium phenocryst assemblages as indicators of magma chamber processes, J. Petrol. 29 (1988) 213–264.
[19] J.P. Davidson, F.J. Tepley III, Z. Palazc, S. Meffan-Main, Magma recharge, contamination and residence times revealed by in situ laser ablation isotopic analysis of feldspar in volcanic rocks, Earth Planet. Sci. Lett. 184 (2001) 427–442.
[20] B.S. Singer, M.A. Dungan, C.D. Layne, Textures and Sr, Ba, Mg, Fe, K, and Ti compositional profiles in volcanic plagioclase: Clues to the dynamics of calc-alkaline magma chambers, Am. Mineral. 80 (1995) 776–798.
[21] R. Wiebe, Plagioclase stratigraphy: A record of magmatic conditions and events in a granitic stock, Am. J. Sci. 266 (1968) 690–703.
[22] K. Stamatelopoulous-Seymour, D. Vlassopoulous, T.H. Pearce, C. Rice, The record of magma chamber processes in plagioclase phenocrysts at Thera volcano, Aegean volcanic arc, Greece, Contrib. Mineral. Petrol. 104 (1990) 73–84.
[23] A.T.J. Anderson, Probable relations between plagioclase zoning and magma dynamics, Fuego Volcano, Guatemala, Am. Mineral. 69 (1984) 660–676.
[24] J.G. Brophy, M.J. Dorias, J. Donnelly-Nolan, B. Singer, Plagioclase zonation in hornblende gabbro inclusions from Little Glass Mountain, Medicine Lake volcano, California: implications for fractionation mechanisms and the formation of composition gaps, Contrib. Mineral. Petrol. 126 (1996) 121–136.
[25] R.A. Wiebe, W.J. Collins, Depositional features and stratigraphic sections in granitic plutons implications for the emplacement and crystallization of granitic magma, J. Sediment. Geol. 20 (1998) 1273–1289.
[26] S.L. Higman, T.H. Pearce, Spatiotemporal dynamics in oscillatory zoned magmatic plagioclase, Geophys. Res. Lett. 20 (1993) 1935–1938.
[27] T.H. Pearce, The analysis of zoning in magmatic crystals with emphasis on olivine, Contrib. Mineral. Petrol. 86 (1984) 149–154.
[28] T.H. Pearce, Recent work on oscillatory zoning in plagioclase, in: I. Parson (Ed.), Feldspars and Their Reactions, Kluwer, London, 1994, pp. 313–349.
[29] M. Cortini, D. Anastasio, Chemical banding in volcanic minerals: a statistical phenomenological aproach, Eur. J. Mineral. 13 (2001) 571–575.
[30] F.J. Tepley III, J.P. Davidson, R.I. Tilling, J.G. Arth, Magma mixing, recharge and eruption histories recorded in plagioclase phenocrysts from El Chichon Volcano, Mexico, J. Petrol. 41 (2000) 1397–1411.
[31] J.P. Davidson, F.J. Tepley III, K.M. Knesel, Isotopic fingerprinting may provide insights into evolution of magmatic systems, EOS Trans. AGU 79 (1998) 185–189.
[32] H. Greenwood, K. McTaggert, Correlation of zones in plagioclase, Am. J. Sci. 255 (1957) 656–666.
[33] T. Holten, B. Jamtveit, P. Meakin, Noise and oscillatory zoning of minerals, Am. Mineral. 64 (2000) 1893–1904.
[34] P. Hoskin, Patterns of chaos: Fractal statistics and the oscillatory chemistry of zircon, Am. Mineral. 64 (2000) 1905–1923.
[35] D. Sibley, T. Vogel, B. Walker, G. Byerly, The origin of oscillatory zoning in plagioclase: A diffusion and growth controlled model, Am. J. Sci. 276 (1976) 275–284.
[36] V.C. Kress, M.S. Ghiorso, Multicomponent diffusion in MgO-Al_2O_3-SiO_2 and CaO-MgO-Al_2O_3-SiO_2 melts, Geochim. Cosmochim. Acta 57 (1993) 4453–4466.
[37] B. Barbarin, Plagioclase xenocrysts and mafic magmatic enclaves in some granitoids of the Sierra Nevada batholith, California, J. Geophys. Res. 95 (1990) 17747–17756.
[38] P. Kumar, E. Foufoula-Georgiou, Wavelet analysis for geophysical applications, Rev. Geophys. 35 (1997) 385–412.
[39] C. Torrence, G.P. Compo, A practical guide to wavelet analysis, Bull. Am. Meteorol. Soc. 79 (1998) 61–78.
[40] S.Y. Bergeron, D.A. Yuen, A.P. Vincent, Looking at the inside of the Earth with 3-D wavelets: a pair of new glasses for geoscientists, Electron. Geosci. 5 (2000) 1–22.
[41] Y. Guyodo, P. Gaillot, J.E.T. Channell, Wavelet analysis of relative geomagnetic paleointensity at OPD Site 983, Earth Planet. Sci. Lett. 184 (2000) 109–123.
[42] C. Piromallo, A.P. Vincent, D.A. Yuen, A. Morelli, Dynamics of the transition zone under Europe inferred from wavelet cross-spectral of seismic tomography, Phys. Earth Planet. Int. 125 (2001) 125–139.
[43] T. Pearce, A. Kolisnik, Observations of plagioclase zoning using interference imaging, Earth Sci. Rev. 29 (1990) 9–26.
[44] G.E. Leblanc, Objective selection of an analysing wavelet function, EOS Trans. AGU 82 (47).

[45] P.V. Danckwerts, The definition and measurement of some characteristics of mixtures, Appl. Sci. Res. A3 (1952) 279–296.
[46] N. Malhotra, I. Mezic, S. Wiggins, Patchiness: A new diagnostic for Lagrangian trajectory analysis in time-dependent fluid flows, Int. J. Bifurcation Chaos 8 (1998) 1053–1093.
[47] J.A. Vazquez, M.R. Reid, Timescales of magmatic evolution by coupling core-to-rim ^{238}U-^{230}Th ages and chemical compositions of mineral zoning in allanite from the youngest Toba Tuff, EOS Trans. AGU 82 (2001) F1350.
[48] J.B. Reid, D.P. Murray, O.D. Hermes, E.J. Steig, Fractional crystallization in granites of the Sierra Nevada: How important is it?, Geology 21 (1993) 587–590.
[49] P.C. Bateman, Plutonism in the Central Part of the Sierra Nevada Batholith, California, USGS Professional Paper 1483, 1992, 183 pp.
[50] R.W. Kistler, B.W. Chappell, D.L. Peck, P.C. Bateman, Isotopic variation in the Tuolumne Intrusive Suite, central Sierra Nevada, California, Contrib. Mineral. Petrol. 94 (1986) 205–220.
[51] P.C. Bateman, B.W. Chappell, Crystallization, fractionation, and solidification of the Tuolumne Intrusive Series, Yosemite National Park, California, Geol. Soc. Am. Bull. 90 (1979) 465–482.
[52] R.W. Kistler, R.J. Fleck, Field Guide for a Transect of the Central Sierra Nevada, California: Geochronology and Isotope Geology, 1994.